Hybrid density functional calculations of the defect properties of ZnO:Rh and ZnO:Ir

David Muñoz Ramo[a,*], Paul D. Bristowe[a]

[a] *Department of Materials Science and Metallurgy, University of Cambridge, Pembroke Street, Cambridge CB2 3QZ, UK.*

Abstract

We report density functional calculations of the atomic and electronic structure of the spinel phases $ZnRh_2O_4$ and $ZnIr_2O_4$ as well as crystalline ZnO lightly doped (1 at.%) with Rh and Ir ions using the B3LYP hybrid functional. Calculations for the spinels show band gaps ($\sim$ 3 eV) and lattice parameters ($\sim$ 2% difference) in reasonable agreement with experimental data. Incorporation of the transition metals into ZnO induces local distortions in the lattice and the appearance of metal *d* levels in the low gap region and near the conduction band minimum, with a *d*-*d* splitting larger than 2 eV, which helps maintain transparency in the material. Addition of a hole to the simulation cell of both spinels and doped ZnO leads to charge localization in the neighbourhood of Rh/Ir accompanied by local lattice deformations to form a small polaron which may lead to low hole mobility. We calculate polaron diffusion barriers in the spinels and obtain values around 0.02-0.03 eV. These very low barrier energies suggest that at high Rh/Ir concentration hole conduction occurs mainly by the band conduction mechanism at room temperature. We also develop models of the amorphous spinels by means of classical molecular dynamics simulations, and observe a marked reduction in the coordination number of Rh/Ir, from 6 to 4, in the amorphous phase, which may reduce transparency in these materials.

1. Introduction

Transparent conducting oxides (TCOs) are characterized by the combination of electrical conductivity approaching that of metals with high transmittance (>80%) in the visible region of the electromagnetic spectrum. *n*-type TCOs like indium tin oxide,[1] indium gallium zinc oxide[2] and many others have been extensively studied.[3] However, the field of *p*-type conductors is still not well developed. Reported *p*-type TCO's show low conductivities when compared

*Corresponding author

Email addresses: dm586@cam.ac.uk (David Muñoz Ramo), pdb1000@cam.ac.uk (Paul D. Bristowe)

with their n-type counterparts,[4] and amorphization of the material further exacerbates the problem.[5] This is due to the low mobility of electrons in the valence band of these materials, which is mainly composed of p orbital states of oxygen. Achieving a good p-type material is essential to be able to manufacture optoelectronic devices with p-n junctions. A new class of p-type zinc oxides with rhodium[5] or iridium[6] has attracted attention recently due to some remarkable features of their electronic structure. In these systems, the gap region is determined by the d bands of Rh/Ir, which are split into a fully occupied t_{2g} band and an unoccupied e_g band due to the octahedral environment in which these cations sit. The t_{2g}-e_g splitting is large enough to permit transparency in these systems. Determining the mechanism of electrical conductivity is a much needed step in order to render these materials applicable for commercial use. In addition, a great deal of interest has been put on the amorphous phases of these materials,[5] as they have the advantage of requiring lower temperatures for deposition on substrates than their crystalline counterparts. Analysis of the impact of amorphization on the electronic structure of these materials is needed to assess possible losses in the performance of devices built using them.

Several theoretical studies have been performed on the spinels $ZnRh_2O_4$ and $ZnIr_2O_4$ in their crystalline phase. Mansourian-Hadavi *et al*[7] analyze the band structure of $ZnRh_2O_4$ using the LDA+U method[8, 9] and conclude that a hole polaron state is likely to be formed in this structure. Nagaraja *et al.*[10] also study this material using GGA+U and the cancellation of nonlinearity method[11] to ensure the correct Koopmans behaviour of the functional, and find that the hole polaron state is unstable. Scanlon *et al.*[12] study the band structure of both $ZnRh_2O_4$ and $ZnIr_2O_4$ spinel structures using the GGA[13] and HSE06[14] functionals and find lack of dispersion in the valence band maximum (VBM)of both materials, suggesting that charge localization is going to be favoured.

In this work, we use the hybrid B3LYP[15, 16] exchange-correlation functional to study the changes induced in the electronic structure of ZnO by the presence of a transition metal M (M=Rh or Ir) in the lattice. We consider two situations: the ZnO structure doped with small amounts of M, and spinels ZnM_2O_4 in which the M content is twice that of Zn. We also look explicitly at hole localization processes in these systems in the framework of p-type conduction. Furthermore, we present a model for the amorphous phase of the ZnM_2O_4 spinels, analyze the local geometry around M and Zn and compare it with that of the crystalline phases.

2. Method

For the *ab initio* calculations, we use the periodic approach and Density Functional Theory (DFT) with a nonlocal density functional. We note that the choice of the functional can be crucial for a correct description of the band gap of the system and of hole localization [17, 18]. The periodic DFT calculations were performed using the CRYSTAL09 package,[19] which uses local basis sets of Gaussian-type orbitals (GTOs), and the hybrid B3LYP functional, as

mentioned previously. This functional was selected after tests on bulk ZnO, $ZnRh_2O_4$ and $ZnIr_2O_4$ proved that it gives values of the band gap and lattice parameters of these systems in good agreement with experimental data, as shown in Table 1. This functional has been used to predict defect properties and charge localization phenomena in ZnO[20], monoclinic HfO_2[21] and ZrO_2,[22] crystalline and amorphous SiO_2,[23, 24] and in other oxides.[25, 26] Oxygen has a basis set consisting of 14s, 6p, and 1d functions contracted to 1s, 3sp, and 1d shells using a 8/411/1 scheme. For the cations, we used relativistic effective core potentials (RECP) to reduce the computational cost. For Zn, we used a Stevens *et al.* RECP [27] that replaces all but 10 valence electrons. The related basis set consists of 8sp and 6d functions contracted to 3sp and 2d shells using a 4211/411 scheme. The Rh RECP was obtained from the database of Hay *et al.* [28] and it replaces all but 17 valence electrons. Its related basis set consists of 5sp and 4d functions contracted to 3sp and 2d shells using a 2111/31 contraction. Finally, a Stevens *et al.* [27] RECP was used for Ir, in which 17 valence electrons are explicitly considered. The basis set for this atom consists of 6sp and 4d functions, contracted to 3sp and 2d shells with a 411/31 scheme.

We considered two types of Zn-M-O system, a dilute supercell and a concentrated supercell. The dilute supercell consists of a 72-atom supercell of ZnO in which one of the Zn atoms has been substituted by M. The concentrated supercell is a 56-atom spinel structure with formula ZnM_2O_4. A Monkhorst-Pack factor of 4 was used for integration in the reciprocal space for each cell, which resulted in a mesh of 36 k points in the irreducible part of the Brillouin zone in all cases. Charge localization is studied by removing one electron in the considered supercell and applying a compensating charge background. In order to facilitate initial hole localization in the spinel supercells, we created small precursor distortions around one particular M site in the supercell. Oxygen atoms near the selected M site have been displaced so as the M-O bonds are shortened by 0.05 Å. The magnitude of the perturbation was selected on the basis of the relaxation around M obtained in the ZnO:M supercells as it is expected to be sufficient for localizing the hole at M and some nearby atoms. We also tried to obtain a localized hole on an O atom of the spinel supercell, but were unable to converge a stable solution.

In order to create a model of the amorphous phases of the Rh and Ir spinels, we performed molecular dynamics (MD) simulations using classical interatomic potentials of the Buckingham form for the Rh/Ir-O interaction, the Zn-O interaction and the O-O interaction. We used the Zn-O and O-O potentials from McCoy et al. [29], and fitted new parameters for the Rh-O and the Ir-O interaction using as starting point the Co-O potentials from the same database. The obtained potentials provide good agreement with the geometry of crystalline M_2O_3 and ZnM_2O_4, with differences between the calculated lattice parameter and the experimental value being around 0.1-2% in the Ir-containing phases and 3-5% in the Rh-containing phases. The polarizability of O atoms was modeled using the shell model of Dick and Overhauser.[30] In order to facilitate the convergence of the MD simulations, O shells and cores have been assigned a nominal mass of 0.994 amu and 15.0 amu respectively. Details of these potentials can be

found in Table 2.

The MD simulations were performed with the DLPOLY code.[31] A rapid quench from the molten state was simulated to obtain the amorphous phase. A time-step of 0.4 fs was employed. The following procedure was implemented to obtain the amorphous phase. The starting point is a cubic supercell of ZnM_2O_4 with 12096 atoms and cell parameter 52.479 Å (Ir) and 50.349 Å (Rh). This supercell was heated to 5000 K for 50 ps in the NVT ensemble, initially using a Berendsen thermostat during the first 10 ps to ensure rapid temperature convergence, then switching to the Nosé-Hoover thermostat. In order to relax the volume of the cell, an additional run of 50 ps in the NPT ensemble using the Nosé-Hoover barostat and thermostat was performed at the same temperature. The resulting structure was cooled from 5000 K to 300 K in a series of 100 fs NPT runs, with temperature being reduced by 10 K between runs. Upon reaching 300 K, the system was equilibrated for an additional 50 ps with data collected over the final 2 ps at 1.2 fs intervals.

3. Results and discussion

3.1. Crystalline Rh-containing phases

We proceed to describe the results of our calculations, including the relaxed geometry of the different M-Zn-O systems and related electronic structure and properties. We start with the dilute ZnO:M supercells. In the case of ZnO:Rh, we observe some significant distortion in the local environment around the Rh atom. The four O atoms surrounding it are displaced away by about 0.1-0.5 Å (see Fig. 1). A fifth oxygen is displaced by about 1 Å towards the Rh atom inducing a fivefold coordination sphere around it with slightly distorted bipyramidal symmetry. This reflects the preference of the Rh ion to have coordination numbers larger than 4, which can be observed in oxides like RhO_2 or Rh_2O_3. The rest of the lattice is largely unaffected by the presence of Rh.

The presence of the Rh in the ZnO supercell induces a series of localized levels of d symmetry in the band gap (see Fig. 2). A series of occupied levels appear at the top of the valence band, between 0.7 eV and 1.8 eV above the VBM. Unoccupied d states are located inside the conduction band, between 1.5 and 1.8 eV above the conduction band minimum (CBM).

Addition of a hole to the supercell induces further relaxation around the Rh atom. One Rh-O bond distance is reduced by about 0.3 Å while the other distances are slightly increased ($\sim$ 0.05 Å). An analysis of the Mulliken charge on each atom shows that most of the hole is localized on Rh, but a significant part (about 30%) is found on the oxygen whose bond to Rh has been shortened (labelled as A* in Fig. 1 (a) and (b)). Occupied d levels are pushed down into the gap; two of them are now just above the VBM, while a third one is located now about 0.8 eV above the VBM. One of the unoccupied d levels in the conduction band is now located just below the CBM, while the other lies 0.8 eV above the CBM.

We focus our attention now on the $ZnRh_2O_4$ spinel. The gap region both at the top of the valence band and the bottom of the conduction band is mainly

composed of the d states of Rh divided in t_{2g} and e_g bands because of the octahedral symmetry around this atom. There also are some small contributions of oxygen p states to the top of the valence band. Like Mansourian-Hadavi *et al.* and Scanlon *et al.*, we find that the top of the valence band shows little dispersion. Addition of a hole into the supercell induces a small polaron in the lattice, which is characterized by charge localization on one Rh atom coupled to lattice distortion in its vicinity. Relaxation is fairly symmetrical, with all Rh-O distances decreasing by about 0.1 Å (see Fig. 3). The rest of the lattice suffers very little perturbation from the presence of the localized hole. Hole localization induces the splitting of an unoccupied level in the one-electron band gap about 0.7 eV above the VBM (see Fig. 4). The presence of this level would effectively reduce the band gap of $ZnRh_2O_4$, and in consequence its transparency would also be reduced. We calculated the self-trapping energy of this polaron as the difference between the energy of the polaron state, and the energy of the hole on the undistorted lattice, and obtained a value of -0.23 eV. This indicates that the polaron state is stable. This value is similar to that found for holes trapped in oxides like HfO_2 and ZrO_2[21, 32]. Our result for polaron stability agrees with the conclusions obtained from the band structure analysis in the work of Mansourian-Hadavi *et al.* [7] and Scanlon *et al* [12], but disagrees with the DFT calculations of Nagaraja *et al.*, which predict that the Rh-centered polaron is unstable.[10]

Creation of a polaron state in $ZnRh_2O_4$ suggests that the main mechanism for hole conduction will be polaron hopping between Rh sites. This may be detrimental to the use of this material as a TCO, as hole mobilities would be very small. In order to investigate the impact of polaron hopping on the overall conduction properties, we calculated the hopping barrier for the shortest diffusion path using a simple linear interpolation scheme. We consider the diffusion of the polaron from Rh atom 1 to a nearest-neighbour Rh atom 2. Then, each point in the diffusion path of the polaron is approximated by weighted averages of the geometries of the polaron in point 1 and the polaron in point 2. With this method we obtain an upper estimate of the real diffusion barrier. The barrier obtained is about 0.03 eV, which is a remarkably small value. This means that, at room temperature, polaron hopping would not be observed experimentally unless the system temperature is lowered. In practical terms, despite the disagreement between our results and those of Nagaraja *et al.* regarding the stability of the self-trapped hole, the conclusion deduced is similar in both cases: polaron hopping will not play a significant role in hole conduction in the conditions at which devices operate.

3.2. Crystalline Ir-containing phases

Ir-containing phases have many similarities to their Rh-containing counterparts. In the case of ZnO doped with Ir, like in ZnO:Rh, O atoms linked to Ir move away, although in this case the displacements are slightly larger, about 0.2 Å. Once again, one O atom in the next-nearest neighbour sphere of Ir shows a large displacement by about 1.0 Å to attach to Ir, increasing its coordination to 5 and creating a slightly distorted bipyramid. Like Rh, Ir induces a series of

localized occupied levels in the gap of ZnO, between 1.3 eV and 2.6 eV above the VBM, and unoccupied levels around 2.0 eV above the CBM (see Fig. 2). Hole addition produces charge localization on Ir, but only slight displacements of the O atoms around it are observed. Occupied Ir levels remain in the band gap, but only at 0.8 eV and 1.6 eV above the CBM, while unoccupied levels are found now about 0.6 eV above the CBM.

In the case of the Ir spinel the gap region is dominated by the Ir states like in the Rh spinel. Our results also agree with Scanlon *et al.* in finding a CBM with large contributions of Ir *s* states instead of *d* states, in contrast with the case of $ZnRh_2O_4$. Addition of a hole also has different behaviour than in the Rh spinel. In this case, the hole is evenly distributed between two nearest-neighbour Ir atoms (see Fig. 3 (d)). We were unable to find a solution for the hole localized on one atom despite trying several precursor local distortions. The distance between these two atoms is reduced by about 0.2 Å, while the surrounding O atoms move slightly to accomodate this new arrangement, although their O-Ir distances hardly change. This localized hole induces an unocuppied level at around 0.8 eV from the VBM (see Fig. 4). Self-trapping energy of this polaron is about -0.51 eV, larger than in the Rh spinel. However, the diffusion barrier calculated by linear interpolation is quite small, about 0.02 eV. Like in the case of the Rh spinel, this result suggests that polaron hopping is going to have negligible impact on the conductivity of the system at room temperature.

3.3. Amorphous $ZnRh_2O_4$ and $ZnIr_2O_4$

Fig. 5 shows the partial radial distribution functions (rdf) of the amorphous structures obtained using the procedure described in the Methods section. In general, the highest peaks in the rdf's are displaced towards shorter distances than in the spinel structure. In the case of the anion-cation distances, the distance is about 0.2-0.4 Å shorter than in the spinel. Differences between distances become larger in the cation-cation case, with values ranging between 0.3-0.5 Å with respect to the spinel. One exception is the M-M distance, which becomes about 0.2-0.3 Å larger than in the spinel. Average coordinations are smaller than those of the crystal. In the Zn-O case, the average is about 0.3 units smaller in $ZnRh_2O_4$ and 0.6 units smaller in $ZnIr_2O_4$. The M-O case is more remarkable, as coordination drops from 6 to less than 4. This result is very different from the structural features proposed from the interpretation of experimental data by Kamiya *et al.* for a-$ZnRh_2O_4$.[5, 33] These authors propose a structure in which RhO_6 octahedra are connected either by the edges or the corners with other octahedra, although the samples studied were partly crystallized. The structure obtained by MD consists mainly of RhO_4 tetrahedra linked to each other through their corners. This may have a noticeable impact in the transparency of the system, as the *d-d* splitting in the gap region of the crystalline phase is heavily influenced by the octahedral environment around M. Conversion to a distorted tetrahedral environment may reduce the band gap and lead to reduced transparency. Further studies using *ab initio* techniques on the obtained geometries are in progress and will be able to clarify this aspect.

4. Conclusions

Ab initio methods show that hole trapping processes take place both in ZnO doped with small amounts of Rh/Ir and in the spinels $ZnRh_2O_4$ and $ZnIr_2O_4$. In the latter case, we have found very small diffusion barriers for hopping of the hole through the lattice. This indicates that hole trapping is not going to play an important role in *p*-type conductivity of these materials. We also propose models of the amorphous phase of these spinels, and observe that the M-O coordination number decreases from 6 to around 4 in both in the Rh- and Ir-containing phases. This change in coordination may have implications for the transparency of the amorphous phases.

5. Acknowledgements

Financial support for this work is provided by the European Commission through contract No. NMP3-LA-2010-246334 (ORAMA).

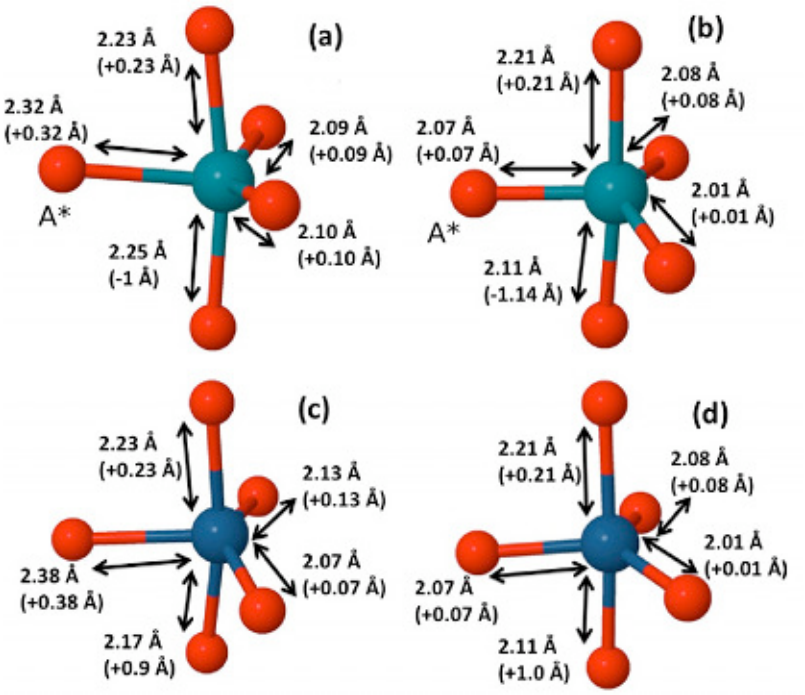

Figure 1: Detail of the geometry around a M atom in the ZnO:M supercell. (a): neutral ZnO:Rh, (b): ZnO:Rh with hole; (c) neutral ZnO:Ir; and (d): ZnO:Ir with hole. Central atom is M, and O atoms are red. Bond distances in parentheses indicate the relaxations caused by the M atom or hole with respect to the perfect ZnO lattice.

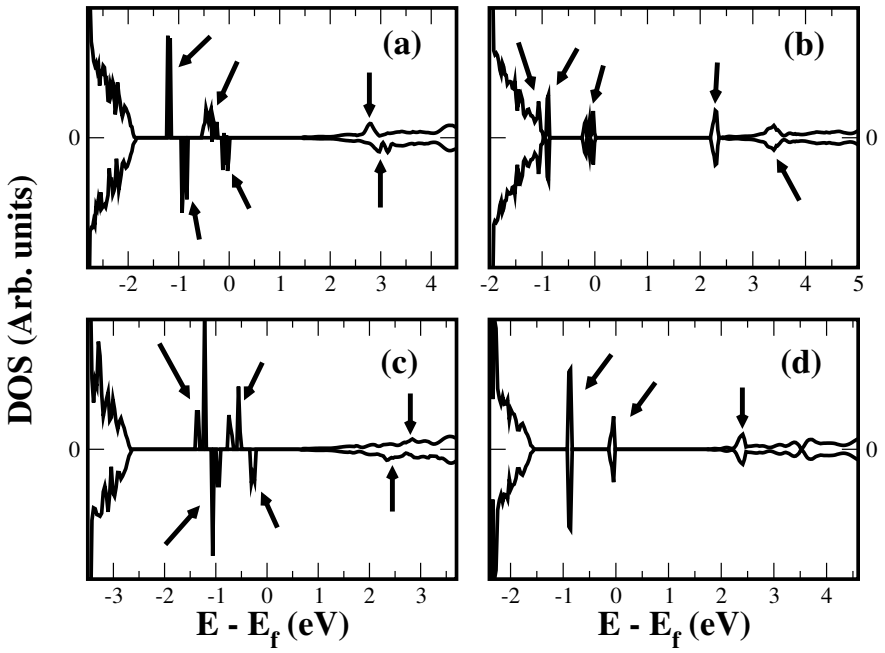

Figure 2: α- and β-spin DOS in the gap region of ZnO:Rh (a), ZnO:Rh with localized hole (b), ZnO:Ir (c), and ZnO:Ir with localized hole (d). Arrows on each graph show the position of d levels in the conduction band corresponding to Rh or Ir.

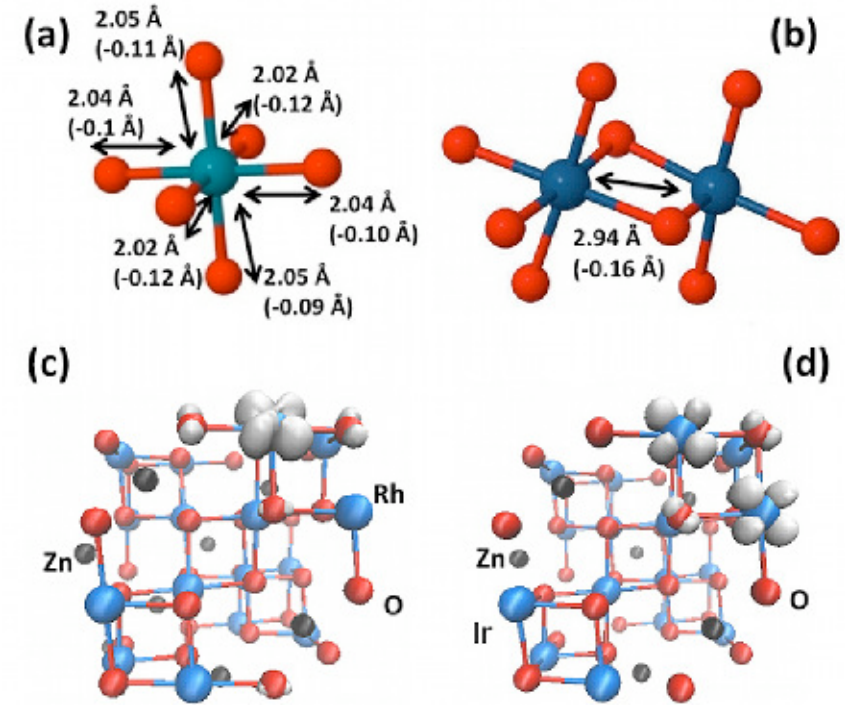

Figure 3: Detail of the geometry and hole localization around a M atom in the ZnM_2O_4 supercells. (a): $ZnRh_2O_4$ with hole, (b): $ZnIr_2O_4$ with hole; (c) spin isosurface (S = 0.01) of the hole distribution in the $ZnRh_2O_4$ supercell; and (d): spin isosurface of the hole distribution in the $ZnIr_2O_4$ supercell (S = 0.01). M atoms are blue, O atoms are red and Zn atoms are black. Spin isosurfaces are shown in grey. Bond distances in parentheses indicate the relaxation caused by the hole.

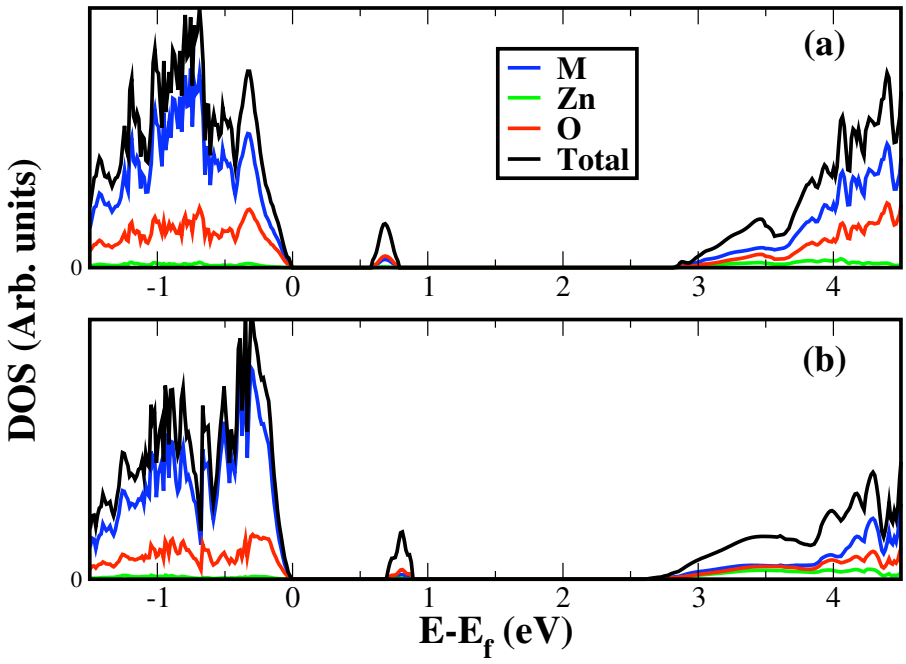

Figure 4: Total and partial DOS in the gap region of $ZnRh_2O_4$ (a) and $ZnIr_2O_4$ (b) with localized hole.

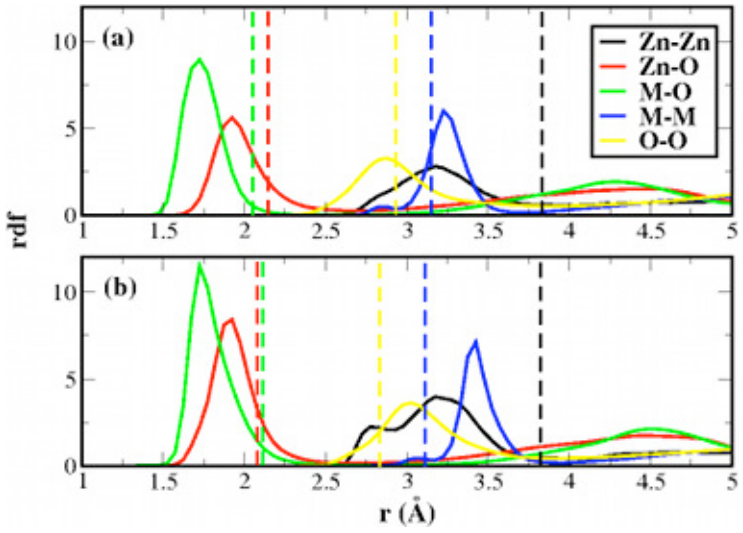

Figure 5: Radial distribution functions for (a) amorphous $ZnRh_2O_4$ and (b) amorphous $ZnIr_2O_4$ from the classical MD simulations. Dashed vertical lines show distances in the crystalline phase calculated with the same interatomic potentials as in the MD simulations.

Table 1: Comparison between band gaps and lattice parameters obtained with B3LYP and experimental data.

		B3LYP	Exp.
ZnO	Band gap (eV)	3.24	3.37[34]
	a(Å)	3.29	3.25[34]
	c(Å)	5.29	5.207[34]
$ZnRh_2O_4$	Band gap (eV)	3.05	2.74[6]
	a(Å)	8.65	8.51[35]
$ZnIr_2O_4$	Band gap (eV)	2.92	2.97[6]
	a(Å)	8.77	8.51[6]

Table 2: Parameters for the M-O interatomic potentials and lattice constants for oxide cells optimized using these potentials. C parameter is zero in both Rh-O and Ir-O potentials. Values in parentheses correspond to the B3LYP calculated lattice constants.

	Rh phases	Ir phases
A (eV)	575.9563	514.6874
ρ (Å)	0.3719	0.3987
M_2O_3 lattice parameters		
a (Å)	4.99 (5.13)	5.28 (5.27)
c (Å)	13.51 (13.85)	14.35 (14.34)
ZnM_2O_4 lattice parameter		
a (Å)	8.39 (8.65)	8.75 (8.77)

References

[1] C. G. Granqvist and A. Hultåker, Thin Sol. Films **411**, 1 (2002).

[2] T. Kamiya, K. Nomura, and H. Hosono, Sci. Technol. Adv. Mater. **11**, 044305 (2010).

[3] P. D. C. King and T. D. Veal, J. Phys.: Condens. Matter **23**, 334214 (2011).

[4] R. Nagarajan, A. D. Draeseke, A. W. Sleight, and J. Tate, J. Appl. Phys. **89**, 8022 (2001).

[5] S. Narushima, H. Mizoguchi, K. Shimizu, K. Ueda, H. Ohta, M. Hirano, T. Kamiya, and H. Hosono, Adv. Mat. **15**, 1409 (2003).

[6] M. Dekkers, G. Rijnders, and D. H. A. Blank, Appl. Phys. Lett. **90**, 021903 (2007).

[7] N. Mansourian-Hadavi, S. Wansom, N. H. Perry, A. R. Nagaraja, and T. O. Mason, Phys. Rev. B **81**, 075112 (2010).

[8] V. I. Anisimov, I. V. Soloyyev, M. A. Korotin, M. T. Czyzyk, and G. A. Sawatzky, Phys. Rev. B **48**, 16929 (1993).

[9] A. I. Liechtenstein, V. I. Anisimov, and J. Zaanen, Phys. Rev. B **52**, R5467 (1995).

[10] A. R. Nagaraja, N. H. Perry, T. O. Mason, Y. Tang, M. Grayson, T. R. Paudel, S. Lany, and A. Zunger, J. Am. Ceram. Soc. **95**, 269 (2012).

[11] S. Lany and A. Zunger, Phys. Rev. B **81**, 205209 (2010).

[12] D. O. Scanlon and G. W. Watson, Phys. Chem. Chem. Phys. **13**, 9667 (2011).

[13] J. P. Perdew, K. Burke, and M. Ernzerhof, Phys. Rev. Lett. **77**, 3865 (1996).

[14] S. Heyd, G. E. Scuseria, and M. Ernzerhof, J. Chem. Phys. **118**, 8207 (2003).

[15] A. D. Becke, J. Chem. Phys. **98**, 1372 (1993).

[16] C. Lee, W. Yang, and R. G. Parr, Phys. Rev. B **37**, 785 (1988).

[17] A. V. Kimmel, P. V. Sushko, and A. L. Shluger, J. Non-Cryst. Solids **353**, 599 (2007).

[18] S. Sicolo, G. Palma, C. Di Valentin, and G. Pacchioni, Phys. Rev. B **76**, 075121 (2007).

[19] R. Dovesi, V. Saunders, C. Roetti, R. Orlando, C. M. Zicovich-Wilson, F. Pascale, B. Civalleri, K. Doll, N. M. Harrison, I. J. Bush, et al., *CRYSTAL09 User's Manual* (University of Torino, 2009).

[20] C. H. Patterson, Phys. Rev. B **74**, 144432 (2006).

[21] D. Muñoz Ramo, A. L. Shluger, J. L. Gavartin, and G. Bersuker, Phys. Rev. Lett. **99**, 155504 (2007).

[22] D. Muñoz Ramo, P. V. Sushko, J. L. Gavartin, and A. L. Shluger, Phys. Rev. B **78**, 235432 (2008).

[23] P. V. Sushko, S. Mukhopadhyay, A. S. Mysovsky, V. B. Sulimov, A. Taga, and A. L. Shluger, J. Phys.: Condens. Matter **17**, S2115 (2005).

[24] L. Giordano, P. V. Sushko, G. Pacchioni, and A. L. Shluger, Phys. Rev. Lett. **99**, 136801 (2007).

[25] F. Cora, M. Alfredsson, G. Mallia, D. S. Middlemiss, W. C. Mackrodt, R. Dovesi, and R. Orlando, Struct. Bond. **113**, 171 (2004).

[26] P. V. Sushko, A. L. Shluger, M. Hirano, and H. Hosono, J. Am. Chem. Soc. **129**, 942 (2007).

[27] W. J. Stevens, M. Krauss, H. Basch, and P. G. Jasien, Can. J. Chem. **70**, 612 (1992).

[28] P. J. Hay and W. R. Wadt, J. Chem. Phys. **82**, 270 (1985).

[29] M. A. McCoy, R. W. Grimes, and W. E. Lee, Philos. Mag. A **76**, 1187 (1997).

[30] B. Dick and A. Overhauser, Phys. Rev. **112**, 90 (1958).

[31] W. Smith and I. T. Todorov, Mol. Sim. **32**, 935 (2006).

[32] K. P. McKenna, M. J. Wolf, A. L. Shluger, S. Lany, and A. Zunger, Phys. Rev. Lett. **108**, 116403 (2012).

[33] T. Kamiya, S. Narushima, H. Mizoguchi, K. Shimizu, K. Ueda, H. Ohta, M. Hirano, and H. Hosono, Adv. Func. Mat. **15**, 968 (2005).

[34] K. Ellmer, A. Klein, and B. Rech, eds., *Transparent Conductive Zinc Oxide: Basics and Applications in Thin Film Solar Cells* (Springer-Verlag, Berlin Heidelberg New York, 2008).

[35] D. J. Singh, R. C. Rai, J. L. Musfeldt, S. Auluck, N. Singh, P. Khalifah, S. McClure, and D. G. Mandrus, Chem. Mater. **18**, 2696 (2006).